RESEARCH PAPER

TiO_2/SiO_2 prepared via facile sol-gel method as an ideal support for green synthesis of Ag nanoparticles using Oenothera biennis extract and their excellent catalytic performance in the reduction of 4-nitrophenol

Bahar Khodadadi [1,2]*

[1] Department of Chemistry, Faculty of Science, University of Qom, Qom, Iran

[2] Center of Environmental Researches, University of Qom, Qom, Iran

ARTICLE INFO

Article History:
Received 18 March 2017
Accepted 29 May 2017
Published 1 July 2017

Keywords:
4-NP
Ag nanoparticles
$NaBH_4$
Oenothera biennis
TiO_2/SiO_2

ABSTRACT

In the present study, the extract of the plant of Oenothera biennis was used to green synthesis of silver nanoparticles (Ag NPs) as an environmentally friendly, simple and low cost method. Additionally, TiO_2/SiO_2 was prepared via facile sol-gel method using starch as an important, naturally abundant organic polymer as an ideal support. The Ag NPs/TiO_2/SiO_2 as an effective catalyst was prepared through reduction of Ag^+ ions using Oenothera biennis extract as the reducing and stabilizing agent and Ag NPs immobilization on TiO_2/SiO_2 surface in the absence of any stabilizer or surfactant. Several techniques such as FT-IR spectroscopy, UV-Vis spectroscopy, X-ray Diffraction (XRD), scanning electron microscopy (FE-SEM), energy dispersive X-ray spectroscopy (EDS), and transmission electron microscopy (TEM) were used to characterize TiO_2/SiO_2, silver nanoparticles (Ag NPs), and Ag NPs/TiO_2/SiO_2. Moreover, the catalytic activity of the Ag NPs/ TiO_2/SiO_2 was investigated in the reduction of 4-nitrophenol (4-NP) at room temperature. On the basis of the results, the Ag NPs/TiO_2/SiO_2 was found to be highly active catalyst according to the experimental results in this study. In addition, Ag NPs/TiO_2/SiO_2 can be recovered and reused several times in the reduction of 4-NP with no significant loss of catalytic activity.

How to cite this article
Khodadadi B. TiO_2/SiO_2 prepared via facile sol-gel method as an ideal support for green synthesis of Ag nanoparticles using Oenothera biennis extract and their excellent catalytic performance in the reduction of 4-nitrophenol. Nanochem Res, 2017; 2(1):140-150. DOI: 10.22036/ncr.2017.01.013

INTRODUCTION

One of the most refractory pollutants in wastewaters is 4-nitrophenol (4-NP), which is generated by industrial sources such as companies manufacturing explosives and dyes [1-4]. It is proven that 4-NP can damage the central nervous system, liver, kidney and blood of humans and animals [1-4].The conventional wastewater treatment methods including adsorption, reverse osmosis, or chemical coagulations cannot be sufficient and effective in the degradation of this compound to non-dangerous product because of their high resistance, high stability and low solubility in water [1-4]. However, 4-NP reduction product, 4-aminophenol (4-AP), is very beneficial and important in various applications as corrosion inhibitor, anti-corrosion lubricant, analgesic and antipyretic drugs, photographic developer, and so on. Therefore, an effective method for 4-NP reduction using metal nano particles has recently received much attention due to its cost effectiveness [4-8]. Owing to their unique physical, chemical, optical and thermodynamical properties, the metal nano particles (MNPs) such as silver NPs have

* Corresponding Author Email: *Khodadadi@qom.ac.ir*

received much attention from researchers for several applications such as gas sensors, catalysis, batteries, high temperature superconductors, solar energy conversion tools, biosensing, antibacterial, antiviral and antifungal activities, drug delivery, etc. [9-14]. Moreover, heterogeneous catalysts are more and more used in the form of the M NPs due to their higher available catalytic surface. Additionally; nano heterogeneous catalysts can make the products easily removable from the reaction mixtures and make the catalysts recyclable [15-17].

However, the agglomeration of the M NPs is a major drawback, which can be overcome with the use of an ideal support. In order to stop the agglomeration of the M NPs and get over the problems associated with their stability, separation, and recovery, several inorganic compounds including zeolite, graphene oxide, TiO_2 and Fe_3O_4 have been applied as M NPs supports [18-20].

Among various supports of heterogeneous catalysts, TiO_2 has been used widely as an efficient support and catalyst in organic reactions. However, to date, there has been no report about TiO_2/SiO_2 as a support. Thus, the present study is reporting replacing TiO_2 by the TiO_2/SiO_2 due to good chemical and thermal stability, different surface chemical properties compared to TiO_2, low cost, low toxicity and excellent optical properties, ease of handling, high photocatalytic activity reusability, and benign character [21, 22].

Up to now, several methods have been employed for the synthesis of TiO_2/SiO_2 nanostructures. Among the various chemical techniques, sol-gel process is a promising method owing to the notable advantages of high purity, good homogeneity, low temperature synthetic conditions, low equipment cost and easily controlled reaction parameters [23, 24]. Hence, in this study, we report a facile sol-gel method to synthesize selected support (TiO_2/SiO_2) using starch as an important, naturally abundant organic polymer for controlling the morphology of nanostructure and preventing agglomeration of samples [24, 25].

Various physical and chemical techniques have been applied in the preparation of the M NPs. However, harsh reaction conditions, the use of expensive, hazardous and toxic capping agents or stabilizers to protect the size and composition of the NPs, high temperature and long reaction times, and low yields of the products are some disadvantages of these methods. Recently, plant extracts have been used as reducing and capping agents in the green synthesis of the M NPs with high yields. These synthetic methods are cost-effective, environmentally friendly, organic solvent-free, easy to work up and suitably scaled up. The potential of different plants as biological materials in the synthesis of the M NPs and their immobilization on different supports is still being explored [14, 15, 26-32]. It is found that the extracts of living organisms act both as reducing and capping agents in the synthesis of nanoparticles. Several plants have been successfully used for efficient and rapid extracellular synthesis of Ag NPs [14-17, 26-32]. The biosynthesis of the Ag NPs using Oenothera biennis extract has not so far been reported.

Oenothera biennis (Fig. 1) is a biennial herbaceous plant commonly known as evening Primroses with a well-established status in pharmaceutical, medicinal, cosmetic, and nutritional applications. Oenothera biennis is widely spread throughout Europe, North America, and Asia. According to the literature, phenolic compounds such as flavonoids and phenol carbonic acids constitute one of the most important groups in Oenothera biennis. Oenothera biennis can be used as an important source for bioreduction of metallic ions and production of nanoparticles [33, 34].

The synthesis of metal or metal oxide NPs using plant extracts has been recently reported. Herein, an environmentally friendly, clean and non-toxic method is reported for the first time for the green synthesis of the Ag NPs/TiO_2/SiO_2 nanocomposites using Oenothera biennis in the absence of any stabilizer or surfactant. The Ag NPs/TiO_2/SiO_2 nanocomposite catalytic activity in the reduction of 4-NP using aqueous $NaBH_4$ has also been studied.

Fig. 1. Image of Oenothera biennis

EXPERIMENTAL

Instruments and reagents

Highly pure chemical reagents were obtained from Merck and Aldrich Chemical Companies. Characterization of the products was carried out by comparison of their physical and spectral data with those of authentic samples. A Nicolet 370 FT/IR spectrophotometer (Thermo Nicolet, USA) was used to record FT-IR spectra using pressed KBr pellets. A Shimadzu UV-2500 double beam spectrophotometer was used to record UV-visible spectra in the wavelength range of 200-700 nm. The sample shapes and sizes were identified by transmission electron microscopy (TEM) using a Zeiss-EM10C operating at an accelerating voltage of 80 kV. A Philips model X'Pert Pro diffractometer was used to carry out X-ray diffraction (XRD) measurements using Cu Kα radiation (λ=1.5418Å) at a scanning rate of 2 °/min in the 2θ range of 10-80˚. A Cam scan MV2300) was used to perform scanning electron microscopy (SEM). EDS (energy dispersive X-ray spectroscopy) performed in SEM was used to determine the measured chemical composition of the prepared nanostructures.

Preparation of TiO_2/SiO_2

In a typical synthesis, samples were prepared by the sol-gel method using the following procedure:

First, 0.2 g of starch was dispersed in absolute ethanol and stirred 10 min using a homogenizer. titanium tetra isopropoxide (TTIP) with molar ratio of TTIP/ethanol = 1.75, was then dissolved in this solution (solution **I**). HNO_3, deionized water, and SiO_2 colloid solution (SiO_2) with molar ratio of ethanol/HNO_3/H_2O/SiO_2 = 43/0.2/1/30 were subsequently dissolved in absolute ethanol (solution **II)**. Finally, solution **II** was added dropwise into solution **I** and the resulting mixture was vigorously stirred for 30 min at room temperature. The obtained transparent colloidal suspension was sonicated for 30 min and aged for 48 h to form a gel. The sample was dried in an oven at 50˚C and ultimately calcinated at 500˚C for 4 hours. All the steps are summarized in Fig. 2.

Preparation of Oenothera biennis extract

10 g of dried, powdered Oenothera biennis were added to 100 mL of 70% (V/V) ethanol solution at 70°C over a period of 45 min, after which the mixture was allowed to cool to room temperature. Then, the extract of Oenothera biennis was centrifuged at 6500 rpm and the supernatant was separated by filtration.

Preparation of the Ag NPs using Oenothera biennis extract

For green synthesis of the Ag NPs, 20 mL of 0.03 M aqueous solution of $AgNO_3$ was added dropwise to 50 mL of Oenothera biennis extract under constant stirring at 80 °C. Reduction of silver ions (Ag^+) to silver (Ag^o) was completed in about 30 min, as monitored by UV-Vis and FT-IR spectra of the reaction mixture**.** The color of the reaction mixture gradually changed in 15 min at 80 °C, indicating the formation of silver nanoparticles. The colored solution of silver nanoparticles was then centrifuged at 6500 rpm for 30 min for complete separation. The obtained precipitate was subsequently washed several times with distilled water and once with ethanol and air dried for 24 h at 50°C in an oven.

Preparation of the Ag NPs/TiO_2/SiO_2

In a typical synthesis of the Ag NPs/TiO_2/SiO_2, 0.5 g of TiO_2/SiO_2 powder was dispersed into 50 mL of Oenothera biennis extract under constant stirring at 80 °C. After 5 min, 20 mL of a 0.03 M aqueous solution of $AgNO_3$ was added dropwise to the extract under constant stirring at 80 °C. The yellow color of the Ag^+ solution immediately changed into dark brown, indicating reduction of Ag^+ to Ag^0 and formation of the Ag NPs. Reduction of silver ions (Ag^+) to silver (Ag^o) was completed in about 30 min, as monitored by UV-Vis and FT-IR spectroscopy. Finally, the solution of the Ag NPs/TiO_2/SiO_2 was centrifuged at 6500 rpm for 30 min for complete separation. The obtained precipitate was then washed several times with distilled water and once with ethanol,

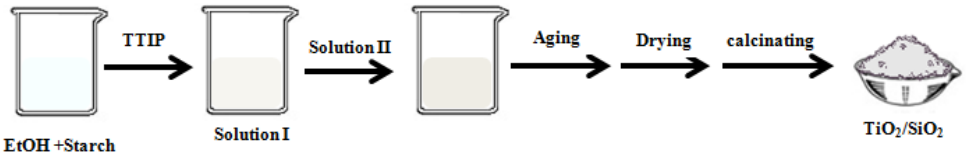

Fig. 2. Diagrammatic synthesis of TiO_2/SiO_2 samples in the presence of starch via sol-gel method

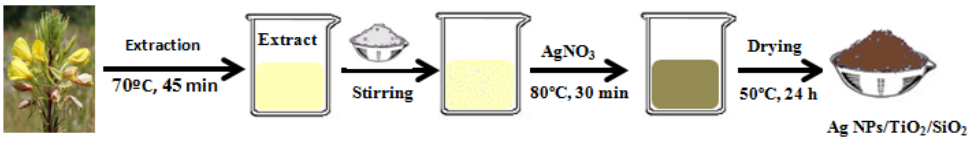

Fig. 3. Diagrammatic synthesis of the Ag NPs/TiO_2/SiO_2 using Oenothera biennis extract

and air dried for 24 h at 50°C in an oven. All the steps are summarized in Fig. 3.

Procedure for the reduction of 4-NP

In typical reduction experiments, the catalytic activity of the Ag NPs/TiO_2/SiO_2 sample was evaluated by the degradation of an aqueous solution of 4-NP. In a typical procedure, 25 mL of the newly prepared sodium borohydride solution (0.25 M) was mixed with 25 mL of 4-NP aqueous solution (2.5 mM) and the mixture was then stirred for 1 min at room temperature. 3.0 mg of the Ag NPs/TiO_2/SiO_2 was subsequently added to the mixture, which was then allowed to stir at room temperature until the deep yellow solution became colorless. The reaction progress was monitored by UV-Vis spectroscopy. The yellow color of the solution gradually vanished, indicating the formation of 4-aminophenol. After completion of reaction, the catalyst was separated from the reaction system by brief centrifugation, washed with ethanol and dried for the next cycle.

RESULTS AND DISCUSSION

Characterization of Oenothera biennis extract and green synthesized Ag NPs

The UV-Vis analysis of Oenothera biennis extract and Ag NPs was performed and the results are shown in Figs. 4 and 5. According to the UV spectrum of Oenothera biennis extract (Fig.4), the two bands at around 283 and 332 nm are assigned to the $\pi \rightarrow \pi^*$ transitions, which can be attributed to the presence of polyphenolics as antioxidants for green synthesis of nanoparticles [34,35]. The reduction of the silver ions (Ag^+) was performed by Oenothera biennis extract. The progression of the reaction and formation of the Ag NPs were controlled by UV-Vis spectroscopy as well (Fig. 5). After completion of the reaction, UV-Vis spectrum showed a maximum absorbance at about 435 nm which can be assigned to the surface plasmon absorption of silver nanoparticles [35- 37].

In order to illustrate the possible functional groups of Oenothera biennis extract and green synthesized Ag NPs using this extract, the FT-IR analysis was performed and results are shown in Figs. 6 and 7. As observed in Fig. 6, Oenothera biennis extract showed some peaks at 3390, 2927 and 1072-1269 cm^{-1}, which are related to OH functional groups, C-H and C-OH stretching vibrations, respectively. Moreover, the absorption band at about 1620 cm^{-1} is due to carbonyl group vibration and the band at 1432 cm^{-1} can be assigned to the stretching C=C aromatic rings [35, 36] Owing to the presence of these functional groups in the structure of polyphenolics, existing in Oenothera biennis extract, it can be concluded that the phenolics in the extract are probably responsible for the reduction of Ag^+ and formation of the corresponding Ag.

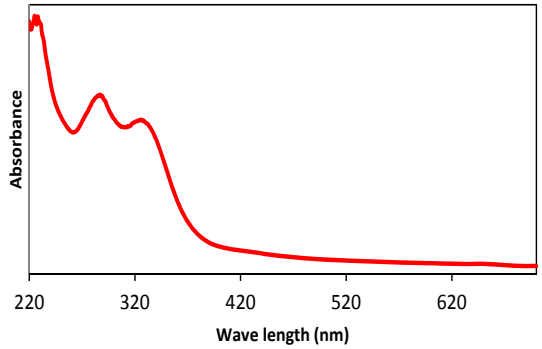

Fig. 4. UV-Vis spectrum of Oenothera biennis extract

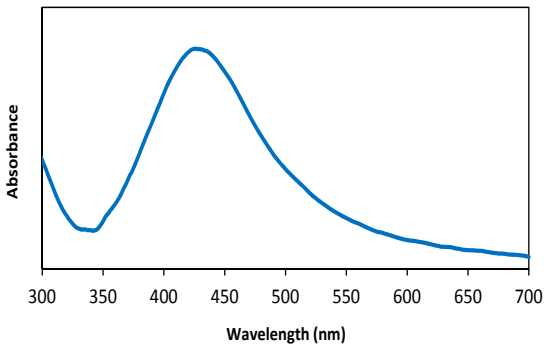

Fig. 5. UV-Vis spectrum of the green synthesized Ag NPs using Oenothera biennis extract

According to the results obtained from the FT-IR study of green synthesized Ag NPs by using Oenothera biennis extract (Fig. 7), the positions of observed peaks are almost similar to those of the corresponding peaks in the FT-IR spectrum of Oenothera biennis extract, showing that the organic compounds in the extract are absorbed on the surface of Ag NPs by π-electron interaction [35]. These results show that the polyphenolics could be adsorbed on the surface of Ag NPs, possibly by interaction through π-electron interaction in the absence of other strong legating agents.

Characterization of TiO_2/SiO_2 and Ag NPs/TiO_2/SiO_2

The chemical structures of TiO_2/SiO_2 and the Ag NPs/TiO_2/SiO_2 were analyzed using Fourier transform infrared (FTIR) spectroscopy at room temperature in the range of 400–4000 cm^{-1} with the composite powder and the results are shown in Fig. 8. It has been reported that in the TiO_2/SiO_2 and Ag NPs/TiO_2/SiO_2 samples, wide absorption bands were observed around 3100-3700 cm^{-1}, due to the OH stretching vibration of surface hydroxyl group because of a great amount of propanol present during the hydrolysis of TTIP [31]. Moreover, physically adsorbed water and hydroxyl group cause absorption bands to appear around 1635 cm^{-1} [39].

The bands at 1117 cm^{-1} in samples correspond to asymmetric stretching vibration of the Ti-O bands [40- 42] and the ones at around 1070-1075 cm^{-1} are due to the symmetrical vibration of the Si-O-Si bands [41- 43]. The peak at 600 cm^{-1} can be assigned to symmetric stretching vibration of the Ti-O-Ti group [44]. Exhibited broad peaks in the range of 400-1000 cm^{-1} are due to the anatase phase [42- 45]. As observed in Fig. 8, in comparison with TiO_2/SiO_2, functional groups have hardly changed after the immobilization of Ag NPs on the surface of TiO_2/SiO_2.

The crystalline structures of the TiO_2/SiO_2 and Ag NPs/TiO_2/SiO_2 samples were examined by X-ray diffraction (XRD) analysis and the results are

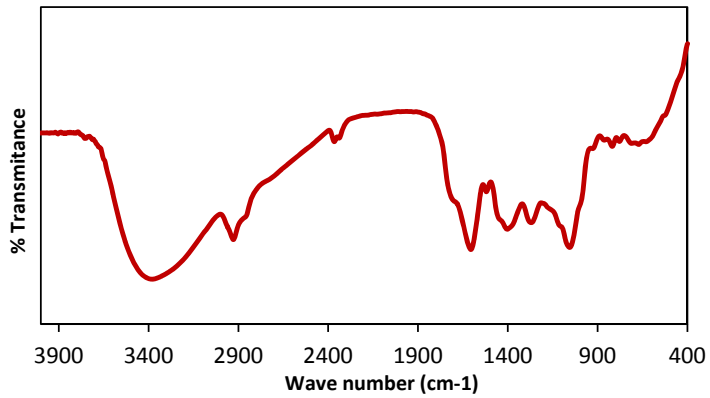

Fig. 6. FT-IR spectrum of Oenothera biennis extract

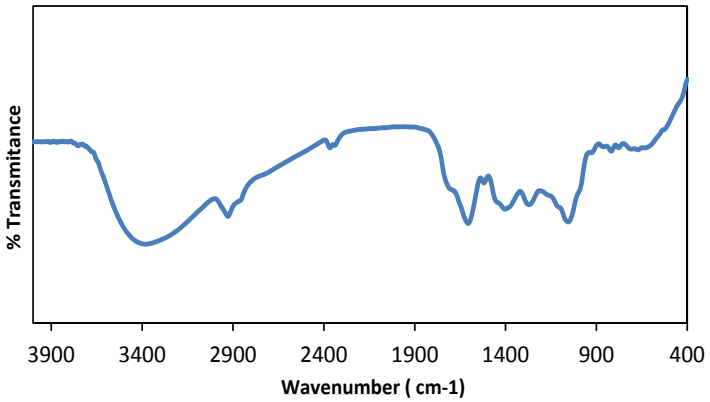

Fig. 7. FT-IR spectrum of the green Ag synthesized NPs using Oenothera biennis extract

shown in Fig. 9.

The diffraction patterns of the TiO_2/SiO_2 sample well match with JCPDS card of TiO_2 (No. 01-080-0074). This pattern of samples can be indexed to that of tetragonal anatase structure phase (the base peak in the range of $20<2\theta<30$ is an evidence of anatase phase). Moreover, diffraction peaks at 25.3, 37.8, 48.2, 55.1, 62.9, 70.5, and 82.9 are assigned to the characteristic anatase phase and those at 27.5, 36.2, 41.5, 45.2, 54.5, 57, and 69.5 are assigned to the characteristic rutile phase [45, 46]. In the meantime, XRD patterns of the TiO_2/SiO_2 sample showed that the anatase phase is dominant.

Fig. 9 shows the XRD pattern of the Ag NPs/TiO_2/SiO_2. On the basis of the above results, the diffraction peaks at 38.73, 44.26, 64.59°, and 78.12° are consistent with the metallic silver particles and well match with JCPDS card of Ag (NO. 04-0783), which exhibits face centered cubic (FCC) structure for the metallic silver NPs immobilized on the surface of TiO_2/SiO_2 without the formation of impurities such as silver oxide (Ag_2O) [35, 36].

Scanning electron microscopy (SEM) analysis was employed to determine the size and morphologies of the Ag NPs/TiO_2/SiO_2 samples. Fig. 10 shows the typical FE-SEM image of the

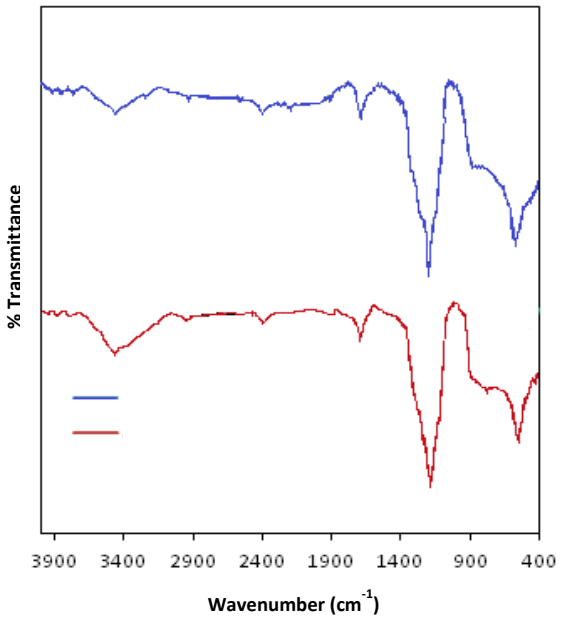

Fig. 8. FT-IR spectrum of the TiO_2/SiO_2 and Ag NPs/TiO_2/SiO_2 samples

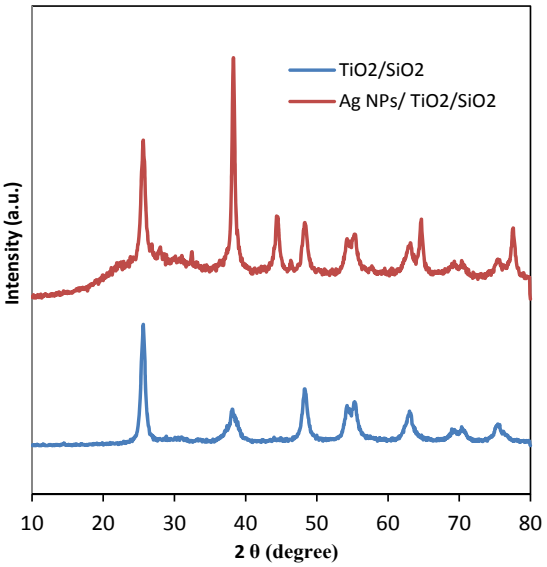

Fig. 9. XRD pattern of the TiO_2/SiO_2 and Ag NPs/TiO_2/SiO_2 samples

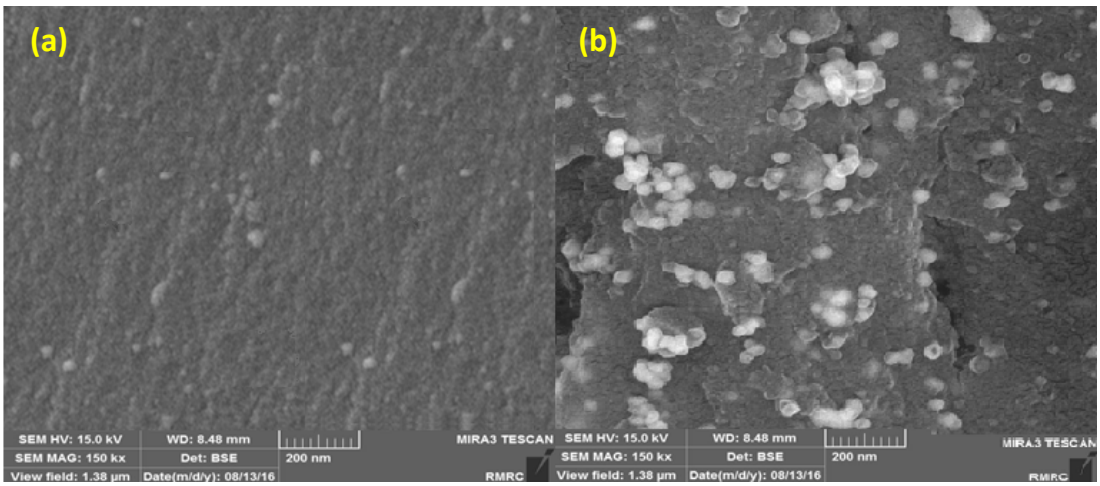

Fig. 10. FE-SEM image of (a) TiO_2/SiO_2 and (b) Ag NPs/TiO_2/SiO_2 samples

samples. These images indicate that TiO_2/SiO_2 and the Ag NPs TiO_2/SiO_2 show spherical morphology with diameters of less than 20 nm with very narrow diameter distributions. From SEM images, it is clear that the Ag NPs are deposited on the surface of TiO_2/SiO_2 without being incorporated in TiO_2/SiO_2.

The elemental composition of Ag NPs/TiO_2/SiO_2 samples was also characterized by EDS spectrum (Fig. 11). Fig. 11 confirms the presence of Ti, O, Si and Ag elements in the Ag NPs/TiO_2/SiO_2 sample.

In order to perform a more detailed study of the morphology and size of the Ag NPs/TiO_2/SiO_2 samples, transmission electron microscopy (TEM) was carried out. Fig. 12 shows the TEM image of typical Ag NPs/TiO_2/SiO_2 samples, in which Ag nanoparticles appear as dark dots over the surface of TiO_2/SiO_2 with average sizes of less than 20 nm.

Catalytic behavior of green synthesized Ag NPs/TiO_2/SiO_2 in the reduction of 4-NP

In this study, the catalytic activity of the Ag NPs/TiO_2/SiO_2 was evaluated in the reduction of 4-NP to 4-AP in the presence of $NaBH_4$. In the absence of the catalyst, the reduction process was not completed in 150 min. The effects of $NaBH_4$ and catalyst concentrations and different amounts of catalyst and $NaBH_4$ on the catalytic reduction of 4-NP to 4-AP were studied and the results are shown in Table 1. According to Table 1, the catalytic efficacy

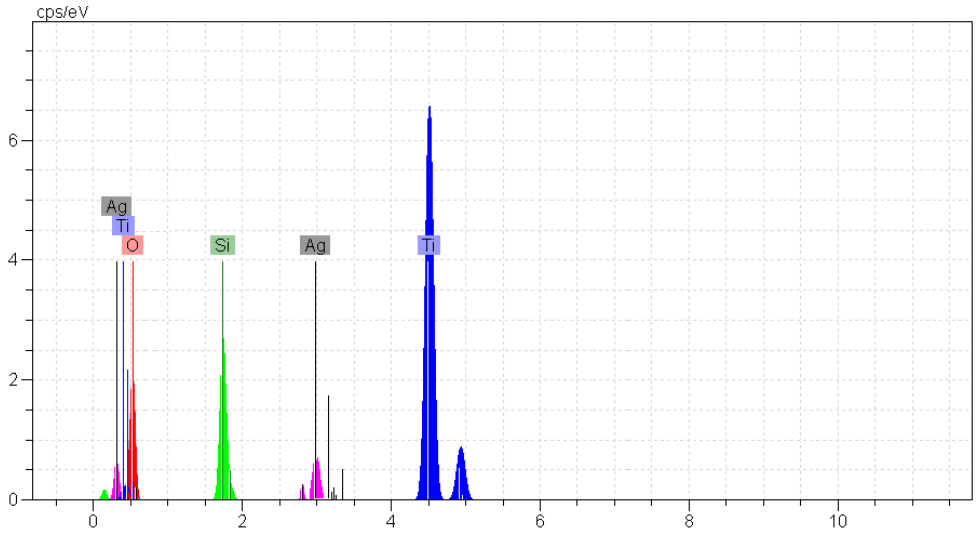

Fig. 11. EDS spectrum of the Ag NPs/TiO_2/SiO_2 sample

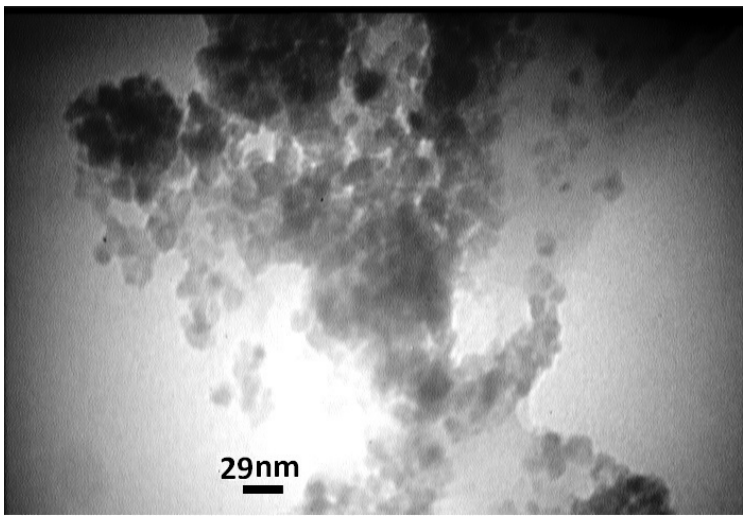

Fig. 12. TEM image of the Ag NPs/TiO_2/SiO_2 sample

increased with an increase in the amount of $NaBH_4$ and catalyst. This means that lower reduction times were observed for higher $NaBH_4$ and Ag NPs/TiO_2/SiO_2 amounts. The best result was obtained using 250 mM (100 equivalents) of $NaBH_4$ and 10.0 mg of catalyst. The reduction process was monitored by using UV-Vis measurements at room temperature and the results are shown in Fig. 13.

According to Fig. 13, after the addition of $NaBH_4$, a red shift of the peak of 4-NP from 315 to 400 nm was observed, owing to alkaline conditions for addition of $NaBH_4$ and formation of 4-nitrophenolate ions. After the addition of catalyst into the reaction system, the reduction process was monitored by using UV-Vis measurements of the reaction mixture. As observed in Scheme 1 and Fig. 13, the absorption peak at 400 nm gradually decreased and disappeared, the solution became clear in the presence of the catalyst and a new peak appeared at about 295 nm, indicating that 4-NP has been converted to 4-AP with increasing the reaction time [35, 36].

It is well known that reduction occurs only in the presence of a catalyst because the catalytic reduction happens on the catalyst surface. Thus, in the absence of a catalyst, no significant reduction process and color change was observed in the reaction.

According to the literature, when the Ag NPs/TiO_2/SiO_2 is used, the BH_4^- ion and 4-NP are both absorbed on the catalyst surface. This can facilitate electron transfer from BH_4^- to 4-NP, leading to 4-AP production. In other words, faster electron transfer can occur on catalyst surface, giving rise to faster reaction. Furthermore, as a support, the TiO_2/SiO_2 prevents the aggregation of Ag NPs, which can play an important role on increasing the catalyst surface and ultimately lowering reduction time.

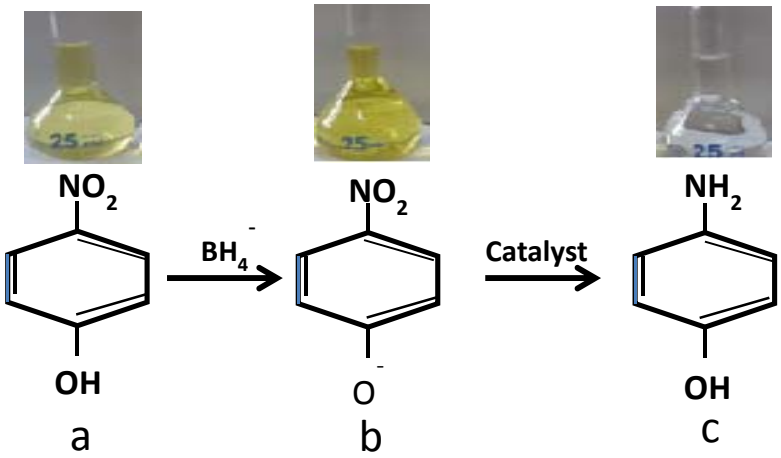

Scheme 1. The reduction reaction of 4-NP to 4-AP

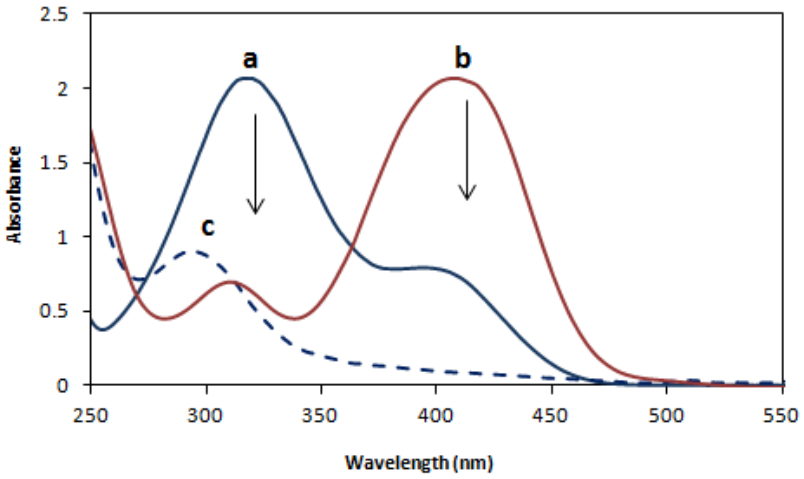

Fig. 13. UV-Vis absorption spectra of 4-NP (a); 4-NP + NaBH4 (b) and 4-AP (c)

Table 1 Completion time for the reduction of 4-NP (2.5 mM) to 4-AP using different amounts of Ag NPs/TiO_2/SiO_2 and $NaBH_4$

	Catalyst (mg)	[$NaBH_4$](mM)	Time (min)
1	3	125	15*
2	3	187.5	9:13
3	3	250	6:58
4	5	125	11:43
5	5	187.5	6:56
6	5	250	5:12
7	7	125	7:49
8	7	187.5	4:21
9	7	250	2:18
10	10	125	3:49
11	10	187.5	2:59
12	10	250	1:32

*: Not completed

Catalyst recyclability

Obviously, recoverability and reusability are the advantages of heterogeneous catalysts; especially for commercial and industrial applications. The recyclability test of the Ag NPs/TiO_2/SiO_2 was also carried out. The Ag NPs/TiO_2/SiO_2 can be easily separated from the reaction mixture by brief centrifugation and multiple washings with distilled water followed by drying. The recovered catalyst was evaluated in the reduction of 4-NP. The catalyst was recycled five times for 100% reduction of 4-nitrophenol, as monitored by UV-Vis spectroscopy. This demonstrates the high stability and catalytic activity of the catalyst under the operating conditions.

CONCLUSIONS

In this article, the Ag NPs and Ag NPs/TiO_2/SiO_2 have been synthesized via an environmentally friendly method using Oenothera biennis extract as reducing agent without any stabilizer or surfactant. Moreover, TiO_2/SiO_2 synthesized via sol-gel method was found to be a valuable support in this regard. The facile synthesis, the application of a plant extract as an economic and effective alternative, cheap, clean, non-toxic and environmentally benign precursor, and the absence of toxic reagents or surfactant templates are some of the remarkable advantages of this method. SEM, XRD, EDS, FT-IR and UV-Vis spectroscopic techniques were used to characterize the synthetic Ag NPs and Ag NPs/TiO_2/SiO_2. Moreover, the Ag NPs/TiO_2/SiO_2 catalytic activity in the reduction of 4-NP using aqueous $NaBH_4$ at room temperature has also been studied. The Ag NPs/TiO_2/SiO_2 has desirable catalytic activity according to the experimental results in this study. In addition, the Ag NPs/TiO_2/SiO_2 nanocomposite could be readily recovered and reused for several cycles in the reduction of 4-NP with almost no loss of catalytic activity.

ACKNOWLEDGMENTS

We gratefully acknowledge the Iranian Nano Council and the University of Qom for the support of this work.

CONFLICT OF INTERESTS

The authors declare that there is no conflict of interests regarding the publication of this paper.

REFERENCES

1. Zhang W, Xiao X, An T, Song Z, Fu J, Sheng G, et al. Kinetics, degradation pathway and reaction mechanism of advanced oxidation of 4-nitrophenol in water by a UV/H2O2 process. Journal of Chemical Technology & Biotechnology. 2003;78(7):788-94.
2. Nakagawa M, Crosby DG. Photodecomposition of nitrofen. Journal of Agricultural and Food Chemistry. 1974;22(5):849-53.
3. Atarod M, Nasrollahzadeh M, Mohammad Sajadi S. Green synthesis of Pd/RGO/Fe3O4 nanocomposite using Withania coagulans leaf extract and its application as magnetically separable and reusable catalyst for the reduction of 4-nitrophenol. Journal of Colloid and Interface Science. 2016;465:249-58.
4. Han Z, Ren L, Cui Z, Chen C, Pan H, Chen J. Ag/ZnO flower heterostructures as a visible-light driven photocatalyst via surface plasmon resonance. Applied Catalysis B: Environmental. 2012;126:298-305.
5. Nasrollahzadeh M, Sajadi SM, Rostami-Vartooni A, Bagherzadeh M, Safari R. Immobilization of copper nanoparticles on perlite: Green synthesis, characterization and catalytic activity on aqueous reduction of 4-nitrophenol. Journal of Molecular Catalysis A: Chemical. 2015;400:22-30.
6. Nasrollahzadeh M, Sajadi SM, Khalaj M. Green synthesis of copper nanoparticles using aqueous extract of the leaves of

Euphorbia esula L and their catalytic activity for ligand-free Ullmann-coupling reaction and reduction of 4-nitrophenol. RSC Advances. 2014;4(88):47313-8.

7. Pozun ZD, Rodenbusch SE, Keller E, Tran K, Tang W, Stevenson KJ, et al. A Systematic Investigation of p-Nitrophenol Reduction by Bimetallic Dendrimer Encapsulated Nanoparticles. The Journal of Physical Chemistry C. 2013;117(15):7598-604.

8. Sivaraj R, Rahman PKSM, Rajiv P, Narendhran S, Venckatesh R. Biosynthesis and characterization of Acalypha indica mediated copper oxide nanoparticles and evaluation of its antimicrobial and anticancer activity. Spectrochimica Acta Part A: Molecular and Biomolecular Spectroscopy. 2014;129:255-8.

9. Nasrollahzadeh M, Sajadi SM, Rostami-Vartooni A, Bagherzadeh M. Green synthesis of Pd/CuO nanoparticles by Theobroma cacao L. seeds extract and their catalytic performance for the reduction of 4-nitrophenol and phosphine-free Heck coupling reaction under aerobic conditions. Journal of Colloid and Interface Science. 2015;448:106-13.

10. Bankar A, Joshi B, Kumar AR, Zinjarde S. Banana peel extract mediated novel route for the synthesis of silver nanoparticles. Colloids and Surfaces A: Physicochemical and Engineering Aspects. 2010;368(1):58-63.

11. Nair LS, Laurencin CT. Silver nanoparticles: synthesis and therapeutic applications. Journal of biomedical nanotechnology. 2007;3(4):301-16.

12. Lee K-S, El-Sayed MA. Gold and Silver Nanoparticles in Sensing and Imaging: Sensitivity of Plasmon Response to Size, Shape, and Metal Composition. The Journal of Physical Chemistry B. 2006;110(39):19220-5.

13. Khodadadi B, Bordbar M, Nasrollahzadeh M. Green synthesis of Pd nanoparticles at Apricot kernel shell substrate using Salvia hydrangea extract: Catalytic activity for reduction of organic dyes. Journal of Colloid and Interface Science. 2017;490:1-10.

14. Khodadadi B, Bordbar M, Nasrollahzadeh M. Achillea millefolium L. extract mediated green synthesis of waste peach kernel shell supported silver nanoparticles: Application of the nanoparticles for catalytic reduction of a variety of dyes in water. Journal of Colloid and Interface Science. 2017;493:85-93.

15. Nasrollahzadeh M, Sajadi SM, Maham M. Green synthesis of palladium nanoparticles using Hippophae rhamnoides Linn leaf extract and their catalytic activity for the Suzuki–Miyaura coupling in water. Journal of Molecular Catalysis A: Chemical. 2015;396:297-303.

16. Petla RK, Vivekanandhan S, Misra M, Mohanty AK, Satyanarayana N. Soybean (Glycine max) leaf extract based green synthesis of palladium nanoparticles. J Biomater Nanobiotechnol. 2012;3(1):14-9.

17. Kurtan U, Baykal A, Sözeri H. Recyclable Fe3O4@Tween20@Ag Nanocatalyst for Catalytic Degradation of Azo Dyes. Journal of Inorganic and Organometallic Polymers and Materials. 2015;25(4):921-9.

18. Nasrollahzadeh M, Mohammad Sajadi S, Rostami-Vartooni A, Khalaj M. Green synthesis of Pd/Fe3O4 nanoparticles using Euphorbia condylocarpa M. bieb root extract and their catalytic applications as magnetically recoverable and stable recyclable catalysts for the phosphine-free Sonogashira and Suzuki coupling reactions. Journal of Molecular Catalysis A: Chemical. 2015;396:31-9.

19. Zargar M, Hamid AA, Bakar FA, Shamsudin MN, Shameli K, Jahanshiri F, et al. Green synthesis and antibacterial effect of silver nanoparticles using Vitex negundo L. Molecules. 2011;16(8):6667-76.

20. Nasrollahzadeh M, Sajadi SM. Synthesis and characterization of titanium dioxide nanoparticles using Euphorbia heteradena Jaub root extract and evaluation of their stability. Ceramics International. 2015;41(10):14435-9.

21. Chen X, Mao SS. Titanium Dioxide Nanomaterials: Synthesis, Properties, Modifications, and Applications. Chemical Reviews. 2007;107(7):2891-959.

22. Khodadadi B, Bordbar M, Yeganeh-Faal A. Optical, structural, and photocatalytic properties of Cd-doped ZnO powders prepared via sol–gel method. Journal of Sol-Gel Science and Technology. 2016;77(3):521-7.

23. Khodadadi B. Facile sol–gel synthesis of Nd, Ce-codoped TiO2 nanoparticle using starch as a green modifier: structural, optical and photocatalytic behaviors. Journal of Sol-Gel Science and Technology. 2016;80(3):793-801.

24. Khodadadi B. Effects of Ag, Nd codoping on structural, optical and photocatalytic properties of TiO2 nanocomposite synthesized via sol-gel method using starch as a green additive. Iranian Journal Catalysis. 2016;6(3):305-11.

25. Taghavi Fardood S, Ramazani A. Green Synthesis and Characterization of Copper Oxide Nanoparticles Using Coffee Powder Extract. Journal of Nanostructures. 2016;6(2):167-71.

26. Fardood ST, Ramazani A, Moradi S. Green synthesis of Ni–Cu–Mg ferrite nanoparticles using tragacanth gum and their use as an efficient catalyst for the synthesis of polyhydroquinoline derivatives. Journal of Sol-Gel Science and Technology. 2017;82(2):432-9.

27. Taghavi Fardood S, Ramazani A, Moradi S, Azimzadeh Asiabi P. Green synthesis of zinc oxide nanoparticles using arabic gum and photocatalytic degradation of direct blue 129 dye under visible light. Journal of Materials Science: Materials in Electronics. 2017.

28. Fardood ST, Atrak K, Ramazani A. Green synthesis using tragacanth gum and characterization of Ni–Cu–Zn ferrite nanoparticles as a magnetically separable photocatalyst for organic dyes degradation from aqueous solution under visible light. Journal of Materials Science: Materials in Electronics. 2017;28(14):10739-46.

29. Taghavi Fardood S, Ramazani A, Golfar Z, Joo SW. Green synthesis of Ni-Cu-Zn ferrite nanoparticles using tragacanth gum and their use as an efficient catalyst for the synthesis of polyhydroquinoline derivatives. Applied Organometallic Chemistry. 2017:e3823-n/a.

30. Khodadadi B, Bordbar M, Yeganeh-Faal A, Nasrollahzadeh M. Green synthesis of Ag nanoparticles/clinoptilolite using Vaccinium macrocarpon fruit extract and its excellent catalytic activity for reduction of organic dyes. Journal of Alloys and Compounds. 2017;719:82-8.

31. Bordbar M, Sharifi-Zarchi Z, Khodadadi B. Green synthesis of copper oxide nanoparticles/clinoptilolite using Rheum palmatum L. root extract: high catalytic activity for reduction of 4-nitro phenol, rhodamine B, and methylene blue. Journal of Sol-Gel Science and Technology.

2017;81(3):724-33.

32. Granica S, Czerwińska ME, Piwowarski JP, Ziaja M, Kiss AK. Chemical Composition, Antioxidative and Anti-Inflammatory Activity of Extracts Prepared from Aerial Parts of Oenothera biennis L. and Oenothera paradoxa Hudziok Obtained after Seeds Cultivation. Journal of Agricultural and Food Chemistry. 2013;61(4):801-10.
33. Ratz-Łyko A, Herman A, Arct J, Pytkowska K. Evaluation of antioxidant and antimicrobial activities of Oenothera biennis, Borago officinalis, and Nigella sativa seedcake extracts. Food Science and Biotechnology. 2014;23(4):1029-36.
34. Rostami-Vartooni A, Nasrollahzadeh M, Alizadeh M. Green synthesis of seashell supported silver nanoparticles using Bunium persicum seeds extract: Application of the particles for catalytic reduction of organic dyes. Journal of Colloid and Interface Science. 2016;470:268-75.
35. Atarod M, Nasrollahzadeh M, Mohammad Sajadi S. Euphorbia heterophylla leaf extract mediated green synthesis of Ag/TiO2 nanocomposite and investigation of its excellent catalytic activity for reduction of variety of dyes in water. Journal of Colloid and Interface Science. 2016;462:272-9.
36. Manonmani V, Juliet V, editors. Biosynthesis of Ag nanoparticles for the detection of pathogenic bacteria in food. Int Conf Innov Manag Serv IPEDR; 2011.
37. Zheng M, Gu M, Jin Y, Jin G. Preparation, structure and properties of TiO2–PVP hybrid films. Materials Science and Engineering: B. 2000;77(1):55-9.
38. Parida KM, Sahu N. Visible light induced photocatalytic activity of rare earth titania nanocomposites. Journal of Molecular Catalysis A: Chemical. 2008;287(1):151-8.
39. Zheng M-p, Gu M-y, Jin Y-p, Wang H-h, Zu P-f, Tao P, et al. Effects of PVP on structure of TiO2 prepared by the sol-gel process. Materials Science and Engineering: B. 2001;87(2):197-201.
40. Jiao J, Xu Q, Li L. Porous TiO2/SiO2 composite prepared using PEG as template direction reagent with assistance of supercritical CO2. Journal of Colloid and Interface Science. 2007;316(2):596-603.
41. Houmard M, Riassetto D, Roussel F, Bourgeois A, Berthomé G, Joud JC, et al. Enhanced persistence of natural super-hydrophilicity in TiO2–SiO2 composite thin films deposited via a sol–gel route. Surface Science. 2008;602(21):3364-74.
42. Khodadadi B, Sabeti M, Nahri-Niknafs B, Moradi-Dehaghi S, Aberomand-Azar P, Raeis-Farshid S. Preparation, characterization and photocatalytic activity of TiO2/CoO nanocomposite. Bulg Chem Commun. 2014;46:624.
43. Khodadadi B. Nickel doping effect on the photocatalytic activity of TiO2/SiO2 nanocomposite. BULGARIAN CHEMICAL COMMUNICATIONS. 2016;48(2):238-43.
44. KHODADADI B. THE INFLUENCE OF AG DOPING ON STRUCTURAL, OPTICAL PROPERTIES AND PHOTOCATALYTIC ACTIVITY OF TIO2/SIO2 NANOCOMPOSITE. Journal of Applied Chemical Research. 2015:119-29.
45. Du J, Wang Z, Zhao G, Qian Y, Chen H, Yang J, et al. Facile synthesis and enhanced photocatalytic activity of porous Sn/Nd-codoped TiO2 monoliths. Microporous and Mesoporous Materials. 2014;195:167-73.
46. . Available from: http://www.epa.gov/ttn/atw/hlthef/nitrophe.html.